Research Article

Nonlinear vibrations of functionally graded cylindrical shell by using numerical analysis in the wave propagation method

M.R. Assari*, A. Kavoosi Nejad and Sh. Amirshirzad

Abstract

Functionally graded materials (FGMs) are materials that show different properties in different areas due to the gradual change of chemical composition, distribution, and orientation, or the size of the reinforcing phase in one or more dimensions. In this paper, the free vibrations of a thin cylindrical shell made of FGM is investigated. In order to investigate this problem, the first-order shear theory is used, by using relations related to the propagation of waves and fluid-structure interaction. Also, due to the rotational inertia of first-order shear deformation and the fluid velocity potential, dynamic equation of functionally graded cylinder shell, containing current is obtained. Convergence of the solutions obtained from this method in different modes of boundary conditions as well as different geometric characteristics for the submerged cylinder and results of other studies and articles is showed. Also the effects of different parameters on the FGM cylindrical shell frequencies for the classical boundary conditions (compositions of simple, clamped, and free boundary conditions) are investigated against the ratio of length to the radius and the ratio of thickness to radius for different values of exponential power (exponential order) of FGM material. The results show that if the more density of the fluid in which the cylinder is submerged is lower, then the frequency values will be higher. Also, by examining the different fluid velocities, it can be seen that the effect of thickness change so that increasing thickness causes the increase of effect of speed on the natural frequency reduction, especially in higher modes.

*Corresponding author
Received 27 June 2019; revised 12 December 2019; accepted 16 April 2020

Mohammad Reza Assari
Department of Mechanical Engineering , Jundi-Shapur University of Technology, Dezful, Iran e-mail: mr_assari@yahoo.com

Ali Kavoosi Nejad
Department of Mechanical Engineering , Jundi-Shapur University of Technology, Dezful, Iran e-mail: Alibox2006@yahoo.com

Shahryar Amirshirzad
Department of Mechanical Engineering , Jundi-Shapur University of Technology, Dezful, Iran e-mail: shahryaramirshirzad@gmail.com

AMS(2010): 76L05.

Keywords: Functionally graded materials; Natural frequencies of cylindrical shell; First-order shear deformation theory; Fluid-structure interaction; Nonlinear vibrations; Propagation method.

1 Introduction

In recent years, with the development of high-powered engines for aerospace industries, turbines, reactors, and other machines, there is a need for materials with higher thermal resistance and more resistant dynamically. Functionally graded materials (FGMs) are in fact composite materials in which the composition of materials or microscopic structure is changed in such a way that the mechanical and thermal properties of the structure made of these materials are ideal for applications that include high thermal gradients from thermal structures in advanced aircraft and aerospace engines and computer circuit boards. According to the many variables that affect the design of FGMs, the full exploitation of the potential of FGMs requires the development of appropriate modeling methods for their response to the combination of mechanical and thermal loads. Emergence and entry of FGMs, by defining the various modes of the existing compounds of human-made, the possibility of the deliberate construction is provided according to these materials. This possibility was proposed as a concept by Bohr and Dowz in 1972, and the exploitation of these materials in individual efforts in the 1950s, 60s, and 70s, and the early 1980s was by many researchers and prominently in the United States. Then Japanese require these materials to grow and progress in space research to focus on the spaceship project that the result was that many of the various hard and precise requirements were made for increasing the temperature of the components of hybrid and gradually microstructural structures; see [25, 19, 4, 11].

Robinson and Palmer [23] carried out a modal analysis of a rectangular sheet suspended on fluid. They obtained the response for a time-harmonic point load, but their analysis can be cited for a limited number of initial frequencies. Kwak [18] examined the free vibration of a rectangular sheet suspended on an infinite fluid. The basis of this analysis is based on the Rayleigh–Ritz method and the Green's function. Haddara and Cao [10] obtained an approximate expansion for the modal analysis of a rectangular sheet of a curved side, horizontally immersed in the fluid, empirically, and analytically. Zhou and Cheung [36] studied the vibrations of a rectangular sheet that is in contact with the fluid in one side, using the Rayleigh–Ritz method. The fluid is in contact with the sheet inside a semi-infinite rigid reservoir. Liang et al. [20] proposed a simple method for obtaining natural frequencies and the shape of the immersed sheet of a clamped side based on

empirical formulas. Yadykin et al. [32] analyzed an immersed rectangular sheet in fluid with ratio of different aspects. The sheets analyzed in their work are with a clamped edge and other edges free. Jeong et al. [15] presented an analytical method for estimating the frequencies of two specific sheets with finite fluid. They used polynomial functions for analysis and satisfied the boundary conditions of the fluid with finite Fourier extension, by expanding the fluid velocity potential. Tarjoman and Carlo [6] studied the sheets of a curved side immersed in fluid and studied the effect of the length-to-width ratio. Zhou and Liu [37] presented a three dimensional method method for dynamically analyzing a flexible rectangular reservoir filled with fluid, using a combination of Rayleigh–Ritz methods and Galerkin's method. FGMs are heterogeneous microstructure materials whose mechanical properties change smoothly and continuously from one surface to another.

The common type is the combination of ceramic and metal. These materials are obtained by mixing ceramic and metal powder. The advantage of using these materials is that they are able to withstand extreme temperatures and temperature differences, and they are extremely corrosion-resistant and have high resistance to fracture. Nowadays, these materials are used for structures that are resistant to high temperatures. This type of materials is used because of its specific features in thermal shields of rockets, chemical tanks, and abrasive environments. Considering the importance of FGMs in the industries, many researchers investigate the dynamic behavior of this type of material. Hosseini-Hashemi et al. [13] investigated and analyzed the free vibration of a rectangular sheet of FGM with a relatively thick based on the first-order shear deformation theory. In their study, for six modes of combining different boundary conditions of a sheet with two simple parallel edges and other edges, a combination of simple, free, and clamped boundary conditions, the natural frequency of the sheet is obtained by using a precise solution. One of the benefits of that research is the high accuracy of the proposed method. Talha and Sinagh [31] studied the vibration and static analysis of FGM sheets using the third-order shear deformation theory, but with the difference that in this theory, little corrections in the transverse displacement of these plates were done by the limited element method. Zhao et al. [35] provided an analysis for the free vibration of the plates of functionally material. They also used the first-order shear deformation theory to calculate shear strain and inertial rotation. The special equations were converted to energy functions using the Ritz method and then solved. Hosseini-Hashemi et al. [12] presented a closed-loop solution based on the free vibration analysis of thick sheets of FGMs based on the third-order shear deformation theory. The boundary conditions used are two simple parallel supports. Khorshidi [16] investigated the effect of the hydrostatic pressure of vibration of a rectangular coupler sheet with a fluid. Ho and Zheng studied the two-branch phenomenon in symmetric nonlinear vibrations of functionally graded circular sheet, considering the effects of temperature and harmonic transverse force. Khorshidi and Farhadi [17] studied the free vibration of rectangular

composite sheet in contact with limited fluid. Abolghasemi et al. [1] ana-lyzed the buckling of rectangular sheets under uneven plate load based on the first-order shear deformation theory and used the Galerkin method for solving equations of stability for a sheet with simple boundary conditions. Ghasemi et al. [8] studied buckling behavior of conical reinforced compos-ite shells under axial load and calculated them by using the Ritz method. Ebrahimi et al. [5] examined the vibrations of FGM beams in thermal load-ing. Guo and Zhang [9] studied on static bending, elastic buckling, and free and forced vibrations, and composite-reinforced fiber structures have been investigated. More recently, Song, Kitipornchai, and Yang [30] examined polymer nanoparticle sheets on the free and compulsory vibrations that op-erate in a categorized manner, in which GPLs are nonuniform and dispersed in matrices. Mirzaei and Kiani [21] examined an iso-geometric formulation for thermal analysis of shaking GRC layers with different compositions in different boundary conditions. They used the assumptions of Shen and his colleagues [26, 29, 27, 28, 33]. Benchouaf and Boutyour [2] studied on the coupled nonlinear static, and dynamic problems were transformed into a se-quence of linear ones solved by a finite-element method. Benferhat et al. [3] studied on the effect of foundation stiffness parameters presented for thick to thin plates and for various values of the gradient index, aspect, and the side-to-thickness ratio.

In this paper, using the first-order shear deformation theory, the vibra-tion of sheets made of FGMs in contact with fluid is studied. In order to examine the displacements and the vibrational behavior of the sheet, the boundary conditions are considered differently. The results are obtained by using the Comsol software for FSI, and in numerical results, different geo-metric conditions, applying fluid to the sheet at various heights, applying different velocities, and obtaining the natural frequencies with checking the different boundary conditions on the natural frequency of the sheet in contact with the fluid with the parametric sweep tool, the effect of volumetric power factor parameters has been investigated and analyzed for several important modes, including the volume ratio and fluid height. To verify the accuracy of the results, numerical results are compared with the results available in references.

2 Statement of the problem

The first step in this research is the modeling of a cylindrical shell consisting of FGM. For this modeling, in the first part, the properties of the materials studied should be considered based on the theories related to FGMs. For this purpose, we consider a cylinder from FGMs with uniform thickness with length L and thickness H and width R that this sheet will consist of ceramic and metal. In all equations, there is the assumption of linear behavior of

materials, displacements, and strains, as well as the elastic properties of materials are in line with the thickness of the variable plate and according to the volume ratio rule. To solve it, using a finite element method, a cylindrical shell model was first drawn in the Comsol software, which is shown in Figure 1 of the cylindrical shell model.
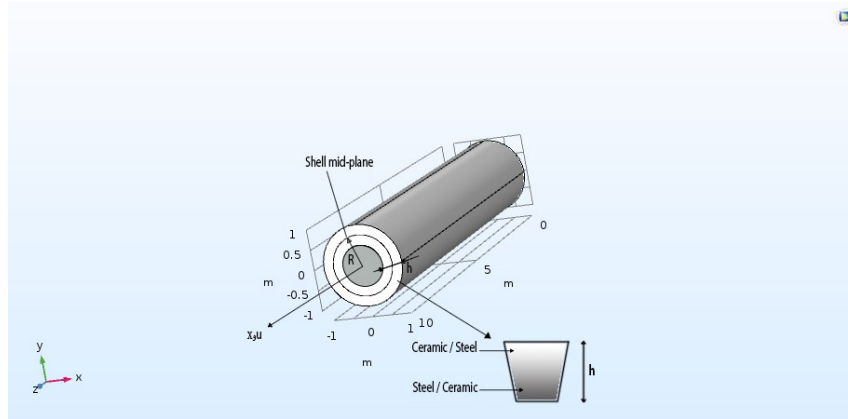

Figure 1: Functionally graded and German cylindrical geometry from cylindrical thickness

The next step in this research is the modeling of the effects of the fluid-structure interaction, which in this paper is modeled by using the coupling motion equations of fluid motion of this interaction. Nonslip and incompressible fluid and the incompressible fluid flow are isotropic and nonrotary. Limited software can be a solution to the condition of observing determinants in the analysis. Thin cylindrical shell is uniformly considered. Equations govern the dynamical behavior of cylinder from the FGM in the presence of fluid.

3 Formulation

The resultant material properties D of an FGM are functions of material properties and volume fractions of the constituent materials and can be modeled as follows (see [14]):

$$D = \sum_{k=1}^{l} D_k V_{fk},$$

where Dk and V_{fk}, respectively, represent the material properties and volume fraction of the constituent material k. The sum of volume fractions of all the constituent materials equals unity, that is,

$$\sum_{k=1}^{l} V_{fk} = 1.$$

For a cylindrical shell with uniform thickness h and with the middle surface taken as reference surface, the volume fraction is expressed as follows (see [14]):

$$V_f = \left(\frac{z}{h} + 0.5\right)^g,$$

where g is the power law index and is taken to be $0 \leq g \leq \infty$. Since the paper study two materials for the construction of a cylindrical shell, three main mechanical quantities, Module Yang (E), Poisson ratio (v), and density (ρ), can be extracted as follows (see [14]):

$$\begin{cases} E_o = (E_2 - E_1)\left(\frac{z}{h} + 0.5\right)^g + E_1, \\ v_o = (v_2 - v_1)\left(\frac{z}{h} + 0.5\right)^g + v_1, \\ \rho_o = (\rho_2 - \rho_1)\left(\frac{z}{h} + 0.5\right)^g + \rho_1. \end{cases}$$

In this case, we know that for $z = -h/2$, the Young's modulus and the Poisson coefficient are, respectively, $v = v_1$ and $E = E_1$, and also the density is equal to $\rho = \rho_1$. When $z = h/2$, Yang modulus and Poisson coefficients are, respectively, $v = v_2$, and $E = E_2$ and also the density is equal to $\rho = \rho_2$, which represents the fact that, at the inner surface of the cylinder, the property of the constituent is corresponding with the first material, and at the outer surface of the cylinder, the mechanical properties are the properties of second material.

The thin sheet problem is a three-dimensional problem which becomes a two-dimensional problem, by considering the plate stress condition. For example, the stress and strain of components in the Z direction are negligible. This theory is used to calculate the effect of shear forces on thick shell frequencies. Using Love's thin shell theory, the equation of motion of this cylindrical shell is shown as follows (see [24]):

$$\begin{cases} \frac{\partial N_x}{\partial x} + \frac{1}{R}\frac{\partial N_{x\theta}}{\partial \theta} = \rho_T \frac{\partial^2 u_x}{\partial t^2}, \\[2mm] \frac{\partial N_{x\theta}}{\partial x} + \frac{1}{R}\frac{\partial N_\theta}{\partial \theta} + \frac{1}{R}\frac{\partial M_{x\theta}}{\partial x} + \frac{1}{R^2}\frac{\partial M_\theta}{\partial \theta} = \rho_T \frac{\partial^2 v}{\partial t^2}, \\[2mm] \frac{\partial^2 M_x}{\partial x^2} + \frac{2}{R}\frac{\partial^2 M_{x\theta}}{\partial x\partial \theta} + \frac{1}{R^2}\frac{\partial^2 M_\theta}{\partial \theta^2} - \frac{N_\theta}{R} = \rho_T \frac{\partial^2 w}{\partial t^2}, \end{cases}$$

where N_x, N_θ, and $N_{x\theta}$ are the force components in the three directions and M_x, M_θ, and $M_{x\theta}$ are the components of the moment in the three main directions. Using the Love's theory for shells, the equations for strains and curves of the reference page will be as follows (see [14]):

$$(N_x, N_\theta, N_{x\theta}) = \int_{-h/2}^{h/2} (\sigma_x, \sigma_\theta, \sigma_{x\theta}) dz,$$

$$(M_x, M_\theta, M_{x\theta}) = \int_{-h/2}^{h/2} (\sigma_x, \sigma_\theta, \sigma_{x\theta}) z dz,$$

$$\rho_o = \int_{-h/2}^{h/2} \rho' dz.$$

There, the Q_{ij}'s are reduced stiffnesses for a thin cylindrical isotropic shell defined as follows (see [14]):

$$Q_{11} = \frac{E}{1 - v^2},$$

$$Q_{22} = \frac{E}{1 - v^2}, \tag{1}$$

$$Q_{12} = \frac{vE}{1 - v^2}, \tag{2}$$

$$Q_{11} = \frac{E}{2(1-v)}.$$

Here E and v, respectively, represent the Young's coefficient and Poisson's coefficient. By placing the above equations in the matrix of force and momentum, we obtain

$$\begin{bmatrix} L_{11} & L_{12} & L_{13} \\ L_{12} & L_{22} & L_{23} \\ L_{31} & L_{31} & L_{31} \end{bmatrix} \begin{bmatrix} u \\ v \\ w \end{bmatrix} = \begin{bmatrix} 0 \\ 0 \\ 0 \end{bmatrix}. \tag{3}$$

In the above equations, $L_{ij}(i, j = 1, 2, 3)$ represents the differential operator relative to x and θ. Since the velocity field for a fluid outside the shell only contains the effect of pressure and no flow outside the tube is observed, using the cylindrical coordinate system (x, φ, r), the acoustic pressure equation satisfies the equation below [24]:

$$\frac{1}{r} \frac{\partial}{\partial r} \left(r \frac{\partial P_a}{\partial r} \right) + \frac{1}{r^2} \frac{\partial^2 P_a}{\partial \varphi^2} + \frac{\partial^2 P_a}{\partial x^2} = \frac{1}{c^2} \frac{\partial^2 P_a}{\partial t^2}. \tag{4}$$

In the upper equation, P_a stands for the acoustic pressure and c indicates the speed of sound inside the water. The coordinates x and φ in the above equations are in accordance with the cylinder coordinates.

In this method, the modal displacement in shell equations can be written by using the wave propagations method and the longitudinal wave number (k_s), as well as by using the parameter of the wave number in the direction of the environment (n) as follows (see [24]):

$$\begin{cases} u\left(x,\theta,t\right) = A\cos\left(n\theta\right)\exp\left(i\omega t - ik_s x\right) , \\ v\left(x,\theta,t\right) = B\sin\left(n\theta\right)\exp\left(i\omega t - ik_s x\right) , \\ w\left(x,\theta,t\right) = C\cos\left(n\theta\right)\exp\left(i\omega t - ik_s x\right) . \end{cases}$$

The coefficients A, B, and C denote the wave amplitudes in the x, θ, and z directions, respectively. In these equations, n is the number of circumferential waves, and k_s is the axial wave number. It should be noted that by changing the boundary conditions, the number of longitudinal waves varies. Also, ω in the above equations shows the natural frequency for the cylindrical shell, and to analyze the waveforms generated, the peripheral wave number is used.

It is assumed that the fluid and shell are in contact at any moment, and the fluid has a flow with velocity U, which will also show the effects of the emission of waves in both fluids.

The associated form of the acoustic pressure field in the contained fluid, which satisfies the acoustic wave (2), can be expressed in the cylindrical coordinate system, associated with an axial wave number k_s, radial wave number k_r, and circumferential wave number n, and is given as follows (see [24]):

$$P = P_a\cos\left(n\theta\right)\,J_n\left(k_r r\right)exp\left(i\omega t - ik_s x\right),$$

where J_n is the Bessel function of first kind with order n. For the fluid outside of the surface and the cylindrical shell, we have (see [24])

$$-\left\{\frac{1}{i\omega\rho_f}\right\}\left(\frac{\partial P_a}{\partial r}\right)\bigg|_{r=R} = \left(\frac{\partial w}{\partial t}\right)\bigg|_{r=R}. \tag{5}$$

Given equation (4) for acoustic pressure, P_a will be obtained by the following equation (see [24]):

$$P_a = \left[\rho_f\omega^2/k_r H_n^{'\,(2)}(Rk_r)\right], \tag{6}$$

where ρ_f is the density of the contained fluid and the prime on the H_n denotes differentiation with respect to the argument Rkr.

Equation (6) represents the amplitude of the acoustic pressure on the shell surface from the fluid outside of the shell and, in other words, determines the effect of the shell's submergence in the fluid.

Using equation (3) and considering the effects of external fluid, (3) could be rewritten as the equation of vibration of the shell as follows (see [22]):

$$\begin{bmatrix} L_{11} & L_{12} & L_{13} \\ L_{12} & L_{22} & L_{23} \\ L_{31} & L_{31} & L_{31} + FL \end{bmatrix} \begin{bmatrix} u \\ v \\ w \end{bmatrix} = \begin{bmatrix} 0 \\ 0 \\ 0 \end{bmatrix}.$$

The FL in the equation above shows the effects of the acoustic pressure due to the submergence of the shell in the fluid. To calculate FL, we have

$$FL_o = -\frac{\rho_f \omega^2}{K_r} \frac{H_n^{(2)}(RK_r)}{H_n'^{(2)}(RK_r)}. \tag{7}$$

In other words, if FL is equal to zero, the equations become vibration equations of a free shell, and in general, the special values of equation (7) represent the natural frequencies of the system.

For the out-tube fluid, by applying the wave propagation method, the equation of wave propagation in the fluid in the tube by using the wave propagation equation for the distribution of pressure is obtained as follows:

$$FL_i = \frac{\rho_f}{K_r} \frac{J_n(RK_r)}{J_n'(RK_r)} \left(\omega^2 - U^2 k_s^2\right). \tag{8}$$

Using (5), (6) can be written as

$$FL = FL_o + FL_i$$
$$= \frac{\rho_f}{k_r}\left(-\frac{H_n^{(2)}(RK_r)}{H_n'^{(2)}(RK_r)}\omega^2 + \frac{J_n(RK_r)}{J_n'(RK_r)}\omega^2 - UK_s\frac{J_n(RK_r)}{J_n'(RK_r)}\right).$$

By (1), we have

$$\begin{bmatrix} T_{11} & T_{12} & T_{13} \\ T_{12} & T_{22} & T_{23} \\ T_{31} & T_{31} & T_{33}+FL \end{bmatrix} \begin{bmatrix} u \\ v \\ w \end{bmatrix} = \begin{bmatrix} o \\ o \\ o \end{bmatrix},$$

where T_{ij} $(i,j = 1,2,3)$ are coefficients of the stiffness matrix and the 3×3 matrix on the right hand side of (6) represents the mass matrix depending on shell parameters and the type of boundary conditions specified at the ends of a cylindrical shell and are given as (see [24])

$$T_{11} = \left[\left(K_s^2\right)A_{11} + \frac{n^2}{R^2}A_{66}\right] - \rho_o h\omega^2,$$

$$T_{12} = \left[-nk_s\left(\frac{A_{11}+A_{66}}{R} + \frac{B_{11}+2B_{66}}{R^2}\right)\right],$$

$$T_{13} = \left[ik_s\left(\frac{A_{12}}{R} + B_{11}k_s^2 + n^2\frac{B_{12}+2B_{66}}{R^2}\right)\right],$$

$$T_{22} = \left[n^2\left(\frac{A_{22}}{R^2} + \frac{2B_{22}}{R^3} + \frac{C_{22}}{R^4}\right) + k_s^2\left(A_{66} + \frac{3B_{66}}{R} + \frac{4C_{66}}{R^2}\right)\right] - \rho_0 h\omega^2,$$

$$T_{23} = \left[-in\left(\frac{A_{22}}{R^2} + \frac{B_{22}}{R^3} + n^2\left(\frac{B_{22}}{R^3} + \frac{C_{22}}{R^4}\right) + k_s^2\left(\frac{B_{12}+2B_{66}}{R^2} + \frac{C_{12}+4C_{66}}{R^2}\right)\right)\right],$$

$$T_{33} = \left[-\left(\frac{A_{22}}{R^2} + \frac{2B_{12}}{R}k_s^2 + 2n^2\frac{B_{22}}{R^3} + C_{11}k_s^4 + 2n^2k_s^2\left(\frac{C_{12}+2C_{22}}{R^2}\right) + n^4\frac{C_{22}}{R^4}\right)\right] - \rho_o h\omega^2.$$

By solving the special value problem for equation (8), the natural frequency of vibration of a thin cylindrical shell can be obtained, by changing n and s, the various vibrational modes of the shell can be obtained.

4 Result and discussion

In this paper, by using two aluminum and ceramic materials (Al2 O3), the mechanical properties of each one are given in Table 1, it is assumed that aluminum will be as an outer coating and ceramic as an inner coating of the sheet that is involved with the fluid.

Table 1: Specification of FGM

Type of material	Density	Elasticity module	Poisson coefficient
Al	2702	70	0.3
Al2 O3	3800	393	0.3

To solve it, using finite element solving method, a cylindrical shell model was first drawn in the software, and then, the problem of structure and fluid interaction was used to consider the effects of the fluid outside and inside the shell. Since in solving a finite element, due to some factors, the response depends on the size of the mesh, it must be ensured that the mesh size is sufficiently small and the dimensions of the mesh have no effect on the solutions. For this purpose, using different mesh sizes, the element solving has been limited. In Figure 2, to show the effect of mesh size on the results of the finite element method for the first frequency, are presented.
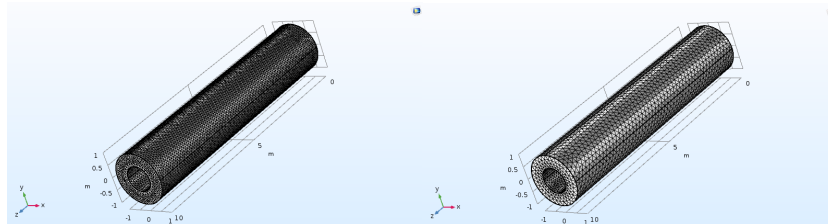

Figure 2: Mesh of cylindrical shell

Because in solving a finite element, due to some factors, the response depends on the size of the mesh, it must be ensured that there is no independence of the mesh network and the dimensions of the mesh do not affect the frequencies. For this purpose, using different sizes of mesh several times, the finite element solving has been performed and the results are presented in Figure 3 for the first frequency.
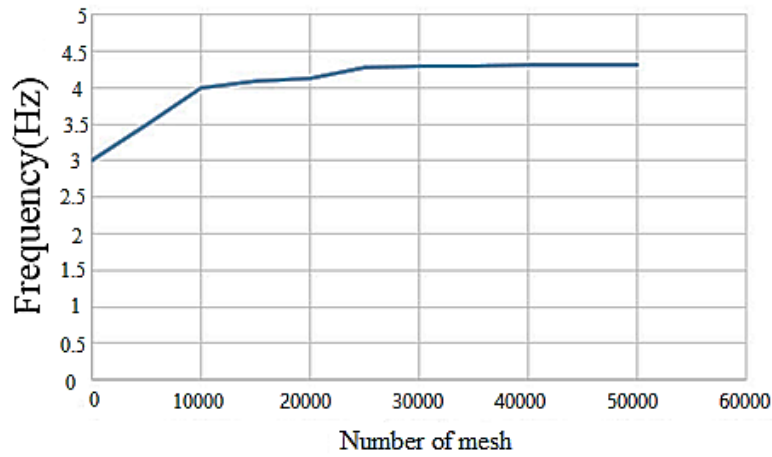
Figure 3: Mesh of cylindrical shell

According to Table 2, the optimal value for solving a finite element in a way that does not depend on the number of meshes, the point of mesh with average element quality is 0.997.

Table 2: Mesh Quality

Mesh shape	Mesh vertices	Number of element	Average element quality
a	70372	387950	0.6643
b	558217	3221150	0.997

After finding the optimal mesh size that has no effect on the solution of the problem, the results for the natural frequency for the form of various modes are presented in Table 3. In Figures 4 and 5, the shape of the vibrational modes associated with the first to third vibrational frequencies in contact with air and in contact with the fluid with fully bounded boundary conditions of the FGM (AL/Al2 O3) with $\alpha= 1$ is shown.

Table 3: The results of the analysis for various figures

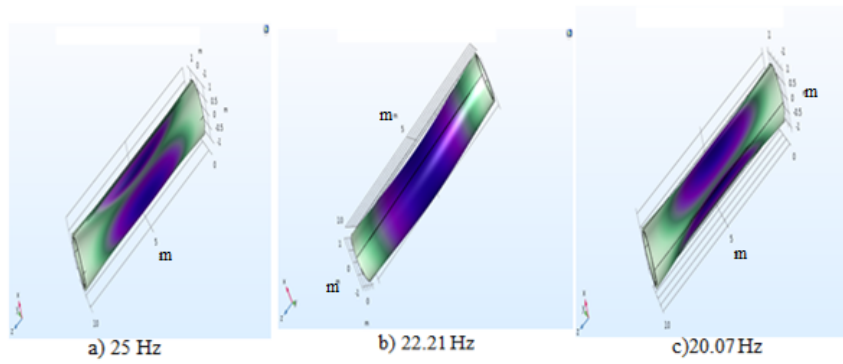| Mode shapes (m,n)	Natural frequency (Hz)
(1,2)	4.53
(1,3)	8.35
(2,3)	11.31
(2,2)	11.53
(1,3)	15.18
(3,3)	20.39
(2,4)	12.51
(3,4)	22.98

Figure 4: Vibrating base frequency variations of FGM in contact with air by clamped boundary conditions
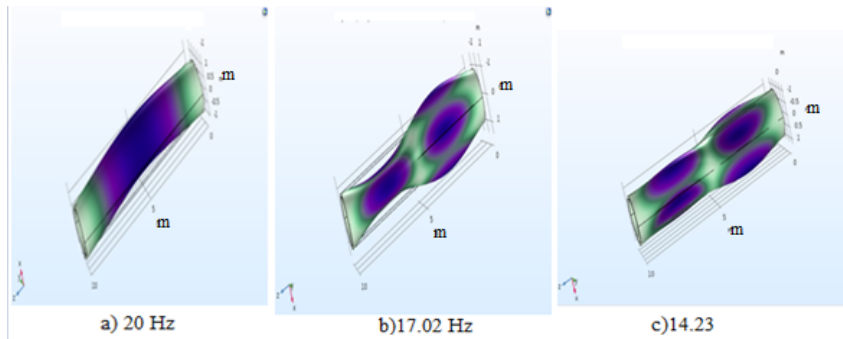

Figure 5: Vibrating base frequency variations of FGM in contact with fluid by clamped boundary conditions

In order to obtain the results of the analysis, with the problem solving, we consider $R = 1m$, $L/R = 15$, and h/R $= 0.005$ and a speed of 1 m/s for the fluid in equation (8). The results is presented in Table 4.

Table 4: Natural frequency in solving software and analytical solution

Mode number	Mode shapes (m, n)	Natural frequency in analytical solution	Natural frequency in solving software
1	(1,2)	5.001	4.92
2	(1,3)	8.71	8.97
3	(2,3)	10.13	11.26
4	(2,2)	10.89	11.42
5	(3,3)	13.85	15.29
6	(1,4)	18.98	20.48
7	(2,4)	20.08	20.57
8	(3,4)	23.01	23.79

As shown in Table 4, in low-frequencies, the results of the analysis of finite element and the analytical results extracted from the above-mentioned method with high accuracy are consistent. In order to better understand the effect of fluid, which is associated with nonrotating flow at a speed of 1 m/s, the comparison between the results of this paper and the results of [7, 14] is presented in Table 5.

Table 5: Comparison of the results of the present study with other similar studies performed in clamped boundary conditions and geometric conditions $L/R = 15$, $h/R = 0.005$, $R = 1m$

Mode number	Mode shapes (m,n)	Natural frequency for fluid contact (submerged cylinder)[14]	Natural frequency for fluid flow inside the tube [7]	Natural frequency for fluid flow with fluid stationary (in this study)
1	(1,2)	5.21	4.93	4.97
2	(1,3)	9.98	8.94	9.31
3	(2,3)	11.36	10.64	10.2
4	(2,2)	11.6	11.48	11.11
5	(3,3)	14.98	14.66	13.64
6	(1,4)	19.01	18.26	17.1
7	(2,4)	19.47	18.73	17.45
8	(3,4)	21.1	19.96	19.1

Given the fact that the fluid velocity can affect the natural vibrational frequencies of the sheet, we consider four different speeds for the fluid. The results for the form of various modes for the geometric conditions $L/R = 15$, $h/R = 0.005$, and $R = 1m$ are shown in table 6.

Table 6: Comparison of natural frequencies for different speeds

Mode number	Mode shapes (m,n)	Natural frequency without speed	Natural frequency for speed 2m/s	Natural frequency for speed 4m/s	Natural frequency for speed 6m/s
1	(1,2)	5.1	5.02	4.58	4.5
2	(1,3)	8.69	9.23	8.61	8.37
3	(2,3)	9.82	9.87	9.77	9.44
4	(2,2)	10.49	10.75	10.23	9.89

In order to better understand the effect of fluid velocity on the natural frequency of the sheet, according to the results of the above table, for different velocities of the fluid, the clamped boundary conditions and the geometric conditions $L/R = 20$, $h/R = 0.002$, and $R = 1m$ for the shape of the various modes in Figure 6 are plotted.
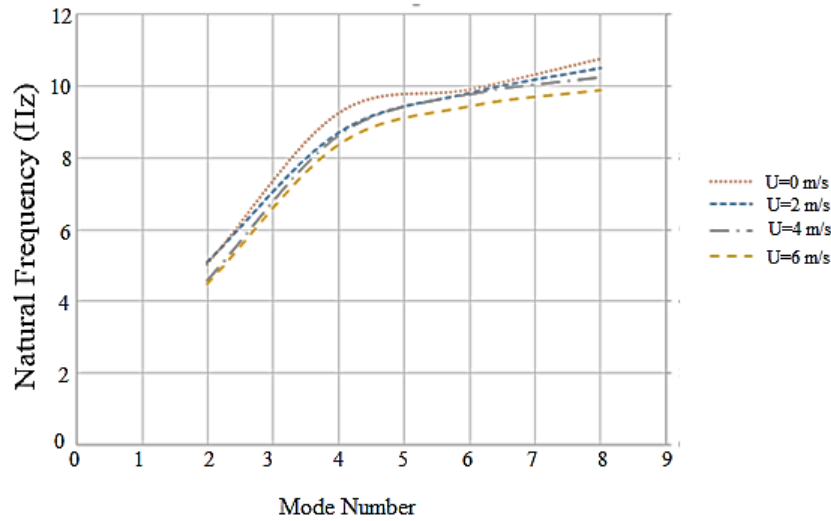

Figure 6: Comparison of the effect of velocity of fluid inside the cylindrical shell on the natural frequency of vibration of shell

As shown in Figure 6, the increase in velocity reduces the natural frequency of the first modes of the shell. It is necessary to note that the effect of the velocity of the fluid on reducing the natural frequencies of the first modes at low velocities is more than high speeds. On the other hand, according to Figure 6, reducing natural frequency in different modes has been done with the change in fluid velocity by approximately one ratio, which can generally be said that increasing the velocity of the fluid in the cylinder reduces the natural frequencies. In other words, it can be expected that by increasing fluid velocity due to increasing fluid dynamic pressure, the con-

nection between the fluid and the structure becomes stronger, which reduces the natural frequencies. This means that the mechanism of the effect of fluid velocity is similar to the mechanism of the effect of fluid and structure continuity, and, likewise [34]. This shows that, considering the effect of the fluid and structure continuity, the natural frequencies of each vibrational mode reduces. Different boundary conditions for free vibration of shell make the numbers of different longitudinal wave. In other words, due to the fact that free vibration of shell must satisfy the boundary conditions (geometric conditions such as displacement, slope, etc.), it is necessary to consider the longitudinal wave number that according to the longitudinal wave number (m), the geometry conditions of the beginning and end of the shell are also realized. According to this issue, it is expected that changing the boundary conditions affects the free vibration of shell.

As shown in Table 7, a change in the boundary conditions makes vibration of sheet undergoing fundamental changes; for this purpose, in the analytical model provided with $U = 2m/s$, the results are as follows:

Table 7: Comparison of the effect of different boundary conditions on natural sheet frequencies in conditions $U = 2m/s$, $L/R = 15$, $h/R = 0.005$, $R = 1m$

Mode number	Mode shapes (m, n)	natural frequencies (HZ)		
		C-C	C-SS	SS-SS
1	(1,2)	5.02	4.66	3.71
2	(1,3)	9.23	7.93	7.18
3	(2,3)	9.89	8.52	6.79
4	(2,2)	10.75	8.95	7.88

As shown in Table 7, different boundary conditions affect the natural frequency of the free vibration of submerged sheet containing fluid flow. According to the results of Table 7,(Clamped-Clamped) C-C mode, which means the clamped boundary conditions for a thin cylindrical shell, the free vibration frequencies have the highest value. In other words, it can be claimed that, by limiting the structure, the first natural frequency will be higher, and consequently, other modes will also have higher frequencies. It is also observed that in (Clamped-Simply Supported) C-SS mode, which means the beam of one side is clamped and one side is simple supported, the natural frequency for each mode is greater than the corresponding mode for the (Simply Supported-Simply Supported) SS-SS mode (simple supported boundary conditions). It should be noted that the SS-SS mode has the least number of constraints among the three modes. It is expected that the flowing fluid shell in this type of boundary condition will require less energy to vibrate, which means that the natural frequencies of free vibrations of the sheet in this case have the least amount than the other boundary conditions. In order to

understand the effect of different boundary conditions on the free vibration frequency, a comparison has been made between different states in Figure 7.
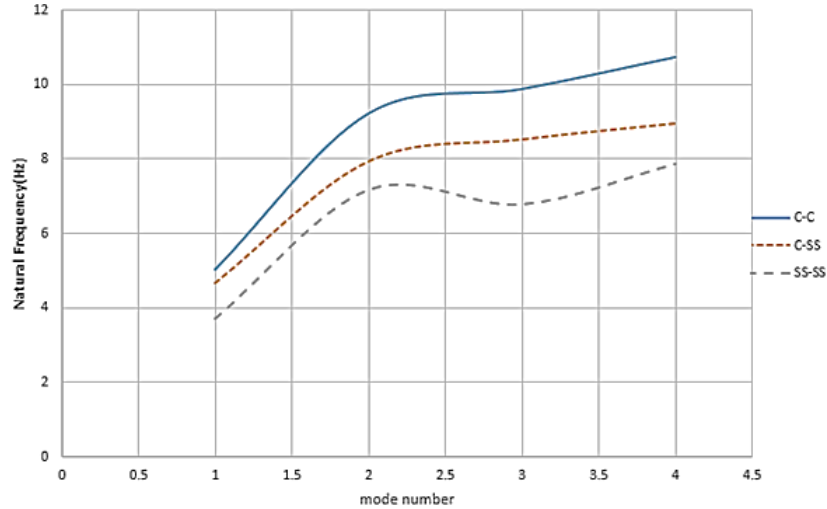

Figure 7: Different boundary conditions $U = 2m/s$, $L/R = 15$, $h/R = 0.005$, $R = 1m$

According to Figure 7, it is concluded that the effect of the SS-SS boundary conditions on the reduction of the natural frequency of sheet vibrations is higher in higher modes. Since the reduction of the natural frequencies of the first vibrational modes has also been observed in other studies due to the change of the boundary conditions of the system from a completely constrain to free state (Iqbal 2009) and (Shah 2011) [14, 24]. According to the results of Figure 7, it can be claimed that in the shell of fluid carrier and submerged in water, the boundary conditions with the number of degrees of constrained release increase the natural frequencies. The main difference observed in this study is that in higher modes, the effect of reducing constraints in boundary conditions on reducing the natural frequency of free shell vibrations is greater than the first and second modes.

Given that the extracted values in the previous sections relate to particular geometric conditions for the shell, it is necessary to examine the effect of geometric parameters on this problem. In the previous sections, parameters $L/R = 15$, $h/R = 0.005$, $R = 1m$ were used. In this section, by changing each of the parameters, the effect of that parameter on the vibrational behavior of the shell is studied. one of the most important geometric parameters is the thickness of the shell, and since in this paper, by assuming the plate stress, the free vibration problem is solved with the wave propagation method, considering the important point that the FGM is used in the structure of this shell, and changes in material from the outer surface to the inner surface are using a shell-thickness function, it can be expected that changing the h/R

ratio affects the natural frequencies of the free vibration of the cylindrical shell.

Table 8: Comparison of the effect of h/R under different velocity conditions of the fluid on the natural frequencies of the structure under conditions of $L/R = 15$ and $R = 1m$

Mode number	Mode shapes (m,n)	$h/R = 0.005$		$h/R = 0.015$		$h/R = 0.03$	
		U=0m/s	U=6m/s	U=0m/s	U=6m/s	U=0m/s	U=6m/s
1	(1,2)	5.1	4.5	9.78	8.23	25.02	19.88
2	(1,3)	8.69	8.37	24.58	23.11	38.98	34.58
3	(2,3)	9.8	9.44	25.01	24.13	40.5	38.8
4	(2,2)	10.49	9.89	35.32	33.58	57.69	47.57

According to Table 8, as expected, the effect of changing the h/R parameter on the natural frequencies of the system is very high, so that it can be said that the fluid velocity change has less effect on the natural frequencies of the cylindrical shell made of FGMs. To understand how affecting the h/R ratio and examining its simultaneous effect with the fluid velocity, Figure 8 is plotted.
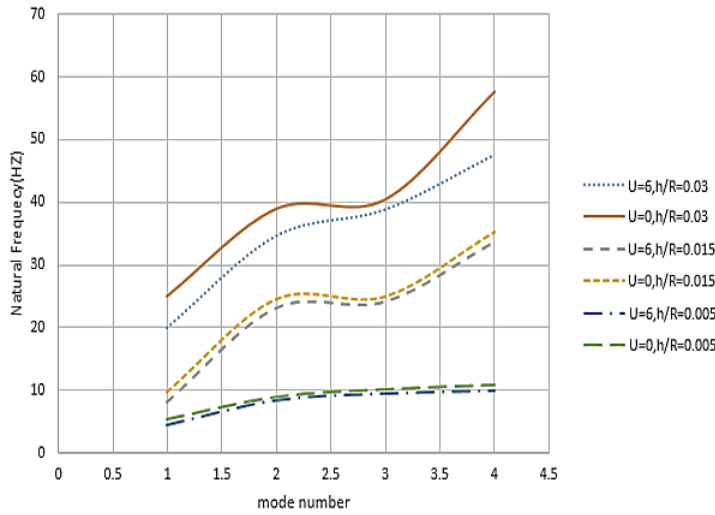

Figure 8: Comparison of the natural frequency of the first modes of sheet under different boundary conditions

Figure 8 shows that by decreasing the h/R ratio, the frequencies also decrease in such a way that at low ratios h/R, by increasing number of modes and a small amount is added to frequency, but in larger values of h/R, by increasing the number of mode and increasing the amount, frequency will

be more. In other words, increasing the h/R ratio will increase the distance between natural frequencies (sequential modes).

In addition, with the increase of h/R ratio, which means increasing the thickness of shell, the natural frequencies of the shell vibration increase, which can be said here, although this problem has been solved for a submerged FGM containing fluid flow, but, as nonemerged isotropic cylinder, the natural frequencies increase by increasing the shell thickness. On the other hand, it can be found from Figure 8 that the increase in the velocity of fluid flow inside the cylindrical shell always has a nearly identical effect on vibrational behavior and by increasing fluid flow due to increasing interaction of the structure and fluid, natural frequencies decrease a little. In addition, the natural frequency variations of the cylinder in contact with the fluid and in contact with air have been discussed in terms of the volumetric power factor.
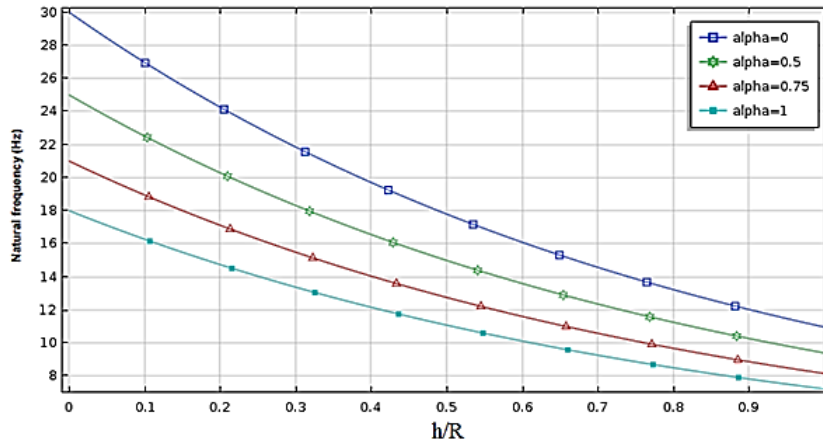

Figure 9: Vibrating base frequency variations of FGM in contact with air in accordance with h/R ratio and four different volumetric ratios with clamped boundary conditions

In Figure 9, the graph of the variations of the vibrating base frequency of sheet from FGM in contact with air with a thickness ratio of $L/R = 15$ and clamped boundary conditions for the power factor of different volume proportions is shown. According to the results presented in the figure above, the more the amount of thickness in the radius increases, the vibration frequency of sheet will be low, and it is also observed that the more the power factor of the volume ratio increases, the frequency of the system also increases. By increasing the volume ratio, the shell rigidity is increased and the ceramic percentage in the sheet increases. The reason is due to the direct relationship between the frequency and the volume ratio in the above figure.
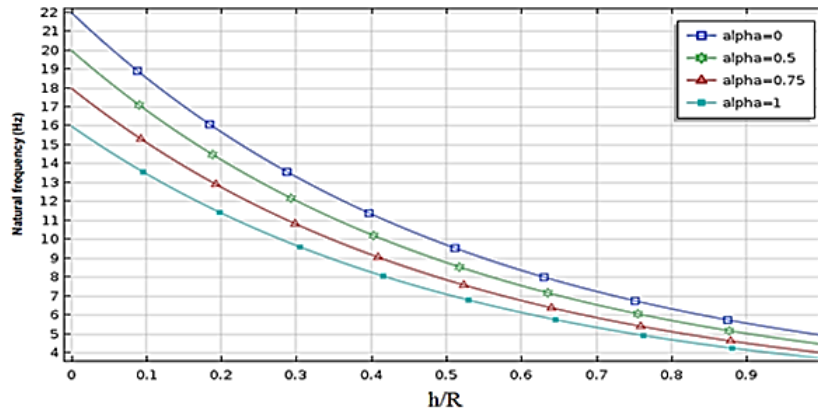
Figure 10: Vibrating base frequency variations of FGM in contact with fluid in accordance with h/R ratio and four different volumetric ratios with clamped boundary conditions

Figure 10 shows the graph of the cylinder base frequency variation from the FGM in contact with the fluid for the power factor of the various volumetric ratios with the clamped boundary conditions. A cylinder with a ratio $L/R = 15$ is in contact with a fluid with a density of $\rho f = 997\,kg/m^3$. First, by comparing the values of the shell frequency in contact with air and fluid, under the same conditions, the frequency in the shell contact with the air is more than the shell's contact state with turbulent fluid. Figure 10 shows that the more the power factor of the volume ratio increases, the system frequency also increases.

5 Conclusions

This paper investigated the free vibration of the cylindrical shell of FGM in contact with turbulent fluid and used first-order shear theory to analyze it. Solving equations related to wave propagation was used to solve the problem of determining free frequencies in a cylindrical shell, which has a structure-fluid interaction. In the fluid inside the shell, because the fluid has a velocity along the longitudinal axis, the potential function was written based on the pressure and velocity of fluid flow. In the case of fluid outside the shell, since shell was considered submerged and fluid constant, solving equations was made by using the hydrostatic pressure. To validate, the analytical results were compared with the results of the analysis by using the Comsol software and the results of other studies. In the boundary conditions, we used three movable simple, non-movable simple, and completely clamped

modes, which were discussed more because of the importance of a completely clamped boundary condition.

Using simulation data provided, the effects of different parameters such as the fluid inside and outside the shell, volume fraction exponent, geometrical parameters, and boundary conditions on the natural frequencies were discussed in detail. The natural frequencies corresponding to the fundamental axial mode number and the smaller values of circumferential wave numbers were strongly affected by the fluid.

By examining the results, a summary of the general conclusion is as follows:

1) Increasing the thickness causes the increase of effect of speed on the reduction of natural frequencies, especially in higher modes.

2) By examining the motion of the fluid at different velocities, it is possible to determine the effect of the thickness change, so that the increase in thickness will increase the effect of speed on the reduction of natural frequencies, especially in higher modes.

3) By increasing the volumetric power factor due to the increase in rigidity of the shell, also the natural frequency increases.

4) The effect of boundary conditions on the free natural frequency was such that, as the constraints increased, the frequency of vibrations also increased, so that the natural frequency in the clamped mode is more than the other two.

5) The natural frequency values of the cylindrical shell in contact with the air are more than contact with the turbulent fluid.

6 Nomenclature

c	speed of sound(m/s)	v	modal displacement Direction θ
H	Thickness(m)	D	Material properties
		V	Volume fraction
E	young modulus(GPa)		Greek letters
k	wave number	ρ'	The mass density of the shell material
M	Moment resultant(N.m)	ρ	Fluid density(kg/m^3)
P	pressure(pa)	α	Poisson ratio
U	Velocity fluid (m/s)	υ	volume ratio
N	Force(N)	ω	natural frequency(Hz)
Q	Reduced Stiffness(N/m)		Subscripts

L	differential operator	i, j	components
A	wave amplitude in the x direction	t	time
B	wave amplitude in the θ direction	f	Contained fluid
C	wave amplitude in the z direction	a	acoustic
r	radius	z	Direction z
n	The number of circumferential waves		
w	modal displacement Direction z	x	Direction x
u	modal displacement Direction x	$x\theta$	Direction $x\theta$
J	Bessel function of first kind	θ	Direction θ
T	Coefficients of the stiffness	o	mass
FL	Effect of acoustic pressure	g	Power law
L	Differential operator	s	axial
ω	Natural frequency of cylindrical shell		

References

1. Abolghasemi, S., Eipakchi, H.R. and Shariati, M. *Analytical solution for buckling of rectangular plates subjected to non-uniform in-plane loading based on first-order shear deformation theory*, Modares Mechanical Engineering, 14 (2015), 37–46.

2. Benchouaf, L. and Boutyour, E.l. *Nonlinear vibrations of buckled plates by an asymptotic numerical method*, Comptes Rendus Mécanique, 344 (2016), 151–166.

3. Benferhat, R., Hassaine Daouadji, T. and Said Mansoura, M. *Free vibration analysis of FG plates resting on an elastic foundation and based on the neutral surface concept using higher-order shear deformation theory*, Comptes Rendus Mécanique, 344 (2016), 631–641.

4. Cherradi, D., Delfosse, B. and Kaw asaki, A. *La Revue de Metallurgie*, CIT, 34 (1996), 185–196.

5. Ebrahimi, F., Ghasemi, F. and Salari, E. *Investigating thermal effects on vibration behavior of temperature-dependent compositionally graded Euler beams with porosities*, Meccanica, 51 (2016), 223–249.

6. Ergin, A. and Urlu B. *Linear vibration analysis of cantilever plates partially Submerged in fluid*, J. Fluid Struct. 17 (2003), 927–939.

7. Farahani, H., Azarafza, R. and Barati, F. *Mechanical buckling of a functionally graded cylindrical shell with axial and circumferential stiffeners using the third-order shear deformation theory*, Comptes Rendus Mécaniqu, 342 (2014), 501–512.

8. Ghasemi, M.A., Yazdani, M. and Soltan Abadi, E. *Buckling behavior investigation of grid stiffened composite conical shells under axial loading*, Modares Mechanical Engineering, 14 (2015), 170–176.

9. Guo, X.Y. and Zhang, W. *Nonlinear vibrations of a reinforced composite plate with carbon nanotubes*, Compos. Struct. 135 (2016), 96–108.

10. Haddara, M.R. and Cao, S. *A study of the dynamic response of submerged Rectangular flat plates*, Mar. Struct. 9 (1996), 913–933.

11. Cahn, R.W., Haasen, P. and Kramer, E.J. *Materials science and technology:A Comprehensive catchment*, Materials Science and Technology, VCH, 1996.

12. Hosseini-Hashemi, Sh., Fadaee M. and Atashipour S.R. *Study on the free vibration of thick functionally graded rectangular plates according to a new exact closed-form procedure*, Compos. Struct. 93 (2011), 722–735.

13. Hosseini-Hashemi, Sh., Rokni-Damavandi-Taher, H., Akhavan, H. and Omidi, M. *Free vibration of functionally graded rectangular plates use first-order shear deformation plate theory*, Appl. Math. Model. 34 (2010), 1276–1291.

14. Igbal, Z., Naeem, M.N. and Sultana, N. *Vibration characteristics of FGM circular cylindrical shells using wave propagation approach*, Acta Mech. (2009), 237–248.

15. Jeong, K.H., Yoo, G.H. and Lee, S.C. *Hydroelastic vibration of two identical rectangular plates*, J. Sound Vib. 272 (2003), 539–555.

16. Khorshidi, K. *Effect of Hydrostatic pressure on vibrating rectangular plates coupled with fluid*, Sci. IRAN. 17 (2010), 415–429.

17. Khorshidi, K. and Farhadi, S. Free vibration analysis of laminated composite rectangular plate in contact with bounded fluid, Compos. Struct. 104 (2013) 176–186.

18. Kwak, M.K. *Hydroelastic vibration of rectangular plates*, J. Appl. Mech. Mar. 63 (1996), 110–115.

19. Leissa, A.W. *Vibration of shells*, NASA SP-288, Reprinted by Acoustical Society of America, America institute of Physics, (1993).

20. Liang, C.C., Liao, C.C., Tai, Y.S. and Lai, W.H. *The free vibration analysis of Submerged cantilever plates*, Ocean Eng. 28 (2001), 1225–1245.

21. Mirzaei, M. and Kiani, Y. *Isogeometric thermal buckling analysis of temperature dependent FG graphene reinforced laminated plates using NURBS formulation*, Compos. Struct. 180 (2017), 606–616.

22. Morse M. and Ingard, K.U. Theoretical Acoustics, Am. J. Phys. 38 (1970), 666–667.

23. Robinson, N.J. and Palmer, S.C. *A modal analysis of a rectangular plate floating On an incompressible liquid*, J. Sound Vib. 142 (1990), 435–460.

24. Shah, G., Mahmood, T., Naeem, M.N. and Arshad, S.H. *Vibration characteristics of fluid-filled cylindrical shells based on elastic foundations*, Acta Mech. 216 (2011), 17–28.

25. Shen, H.S. and Chen, T.Y. *Buckling and postbuckling behavior of cylindrical shells under combined external pressure and axial compression*, Thin-Walled Struct. 12 (1991), 321–334.

26. Shen, H.S., Xiang, Y. and Lin, F. *Nonlinear bending of functionally graded graphene-reinforced composite laminated plates resting on elastic foundations in thermal environments*, Compos. Struct. 170 (2017), 80–90.

27. Shen, H.S., Xiang, Y. and Lin, F. *Nonlinear vibration of functionally graded graphene-reinforced composite laminated plates in thermal environments*, Comput. Methods Appl. Mech. Eneg. 319 (2017), 175–193.

28. Shen, H.S., Xiang, Y. and Lin, F. *Thermal buckling and postbuckling of functionally graded graphene-reinforced composite laminated plates resting on elastic foundations*, Thin-Walled Struct. 118 (2017), 229–237.

29. Shen, H.S., Xiang, Y., Lin, F. and D. Hui, *Buckling and postbuckling of functionally graded graphene-reinforced composite laminated plates in thermal environments*, Composites, 119 (2017), 67–78.

30. Song, M., Kitipornchai, S. and Yang, J. *Free and forced vibrations of functionally graded polymer composite plates reinforced with graphene nanoplatelets*, Compos. Struct. 159 (2017), 579–588.

31. Talha, M. and Singh, B.N. *Static response and free vibration analysis of FGM Plates using higher order shear deformation theory*, Appl. Math. Model. 34 (2009), 3991–4011.

32. Yadykin, Y., Tenetov, V. and Levin, D. *The added mass of flexible plate oscillating in fluid*, J. Fluids Struct. 17 (2003), 115–123.

33. Yu, Y., Shen, H.S., Wang, H. and Hui, D. *Postbuckling of sandwich plates with grapheme reinforced composite face sheets in thermal environments*, Compos. B. Eng. 135 (2018), 72–83.

34. Zhang, X.M., Liu, G.R. and Lam K.Y. , *Vibration analysis of thin cylindrical shells using wave propagation approach*, J. Sound Vib. 239 (2001), 397–403.

35. Zhao, X., Lee, Y.Y. and Liew, K.M. *Free vibration analysis of functionally graded plates using the element-free kp-Ritz method*, J. Sound Vib. 319 (2009), 918–939.

36. Zhou, D. and Cheung, Y.K. *Vibration of vertical rectangular plate in contact with water on one side*, Earthq. Eng. Struct. Dyn. 29 (2000), 693–710.

37. Zhou, D. and Liu, W. *Hydroelastic vibrations of flexible rectangular tanks partially filled with liquid*, Int. J. Numer. Meth. Eng. 71 (2007), 149–174.